Front. Earth Sci. 2014, 8(3): 405–413
DOI 10.1007/s11707-014-0432-0

RESEARCH ARTICLE

Sensitivity analysis for leaf area index (LAI) estimation from CHRIS/PROBA data

Jianjun CAO[1,2], Zhujun GU (✉)[2], Jianhua XU[1], Yushan DUAN[1], Yongmei LIU[2], Yongjuan LIU[2], Dongliang LI[2]

1 The Key Laboratory of GIScience of the Education Ministry PRC, East China Normal University, Shanghai 200062, China
2 School of Bio-chemical and Environmental Engineering, Nanjing Xiaozhuang University, Nanjing 211171, China

Abstract Sensitivity analyses were conducted for the retrieval of vegetation leaf area index (LAI) from multi-angular imageries in this study. Five spectral vegetation indices (VIs) were derived from Compact High Resolution Imaging Spectrometer onboard the Project for On Board Autonomy (CHRIS/PROBA) images, and were related to LAI, acquired from *in situ* measurement in Jiangxi Province, China, for five vegetation communities. The sensitivity of LAI retrieval to the variation of VIs from different observation angles was evaluated using the ratio of the slope of the best-fit linear VI-LAI model to its root mean squared error. Results show that both the sensitivity and reliability of VI-LAI models are influenced by the heterogeneity of vegetation communities, and that performance of vegetation indices in LAI estimation varies along observation angles. The VI-LAI models are more reliable for tall trees than for low growing shrub-grasses and also for forests with broad leaf trees than for coniferous forest. The greater the tree height and leaf size, the higher the sensitivity. Forests with broad-leaf trees have higher sensitivities, especially at oblique angles, while relatively simple-structured coniferous forests, shrubs, and grasses show similar sensitivities at all angles. The multi-angular soil and/or atmospheric parameter adjustments will hopefully improve the performance of VIs in LAI estimation, which will require further investigation.

Keywords CHRIS/PROBA, LAI, sensitivity, vegetation index, vegetation type

1 Introduction

Vegetation structure, a concept describing vegetation spatial and temporal distributions, is very important for environmental research, climate change monitoring and natural resources management. Many factors are sensitive to vegetation structure, including biodiversity, hydrologic cycle, ground energy flux exchange, and carbon storage in land ecosystems (Smith et al., 2008; Ganguly et al., 2008; Fernández et al., 2010; Wu et al., 2014). Leaf area index (LAI), one of many vegetation structure measurements, defined as one-sided surface area of leaves per unit ground area (Chen and Black, 1992), is the key biophysical variable influencing land surface photosynthesis, transpiration, and energy balance (Running et al., 1989; Bonan, 1995).

LAI measurements are traditionally undertaken by acquisitions of vegetation area on the ground (e.g., Duan, 1996), or by the measurement of solar radiance under vegetation using various instruments (e.g., Gower et al., 1999; Hyer and Goetz, 2004). Direct measurement of LAI is usually labor intensive, impractical at large scales, and problematic for capturing seasonal or annual variations. Remote sensing techniques provide a means of quickly estimating LAI in local or global regions. The methods for remotely estimating the LAI are generally grouped into two main classes. One utilizes radiative transfer models to derive the LAI via inversion techniques (Houborg et al., 2007; Darvishzadeh et al., 2008; Vohland et al., 2010). Even though the models are mechanism-based, selection of the model parameters is not straightforward, and inversion is often time-consuming. The other is based on empirical relationships between vegetation indices (VI) derived from satellite data and LAI acquired through field measurement. These empirical models can easily be built and therefore, have been universally applied in LAI estimation over long periods of time (Baret and Guyot, 1991; Chen et al., 2002; Cohen et al., 2003; Fernandes et al., 2003; Gu et al., 2012). Regression models are based on the experimental relationships between combinations of reflectance in different spectral bands and the parameter to be retrieved. The

Received May 31, 2013; accepted December 8, 2013

E-mail: zhujungu@163.com

general applicability of the empirical approaches is reduced because the VIs are affected by many factors, including saturation at high forest cover, atmosphere, leaf structure, canopy geometry, vegetation developmental stage, geometry of observation, and understory backgrounds. In a variety of empirical models, angular information was usually ignored, and the remote sensing data reported were mostly based on the near zenith angle. Colombo et al. (2003) derived spectral VIs from IKONOS data to retrieve LAI of agricultural crops in the S. Colombano region, Italy, and showed that the relationships between spectral VIs and LAI should be developed separately for each vegetation type. McAllister and Valeo (2007) used three methods of linear spectral mixture analysis, modification of spectral VIs, and normalized distance to estimate LAI from a SPOT-4 image in Kananaskis Country, Canada. They concluded that all methods exhibited varying degrees of performance and demonstrated significant dependence on vegetation type. Gu et al. (2011) used a SPOT-5 image to derive six spectral vegetation indices from four radiometric correction levels, which was then related to *in situ* measured LAI in Fujian Province, China. They reported that the use of multiple radiometric correction images can better exploit the capabilities of remote sensing information in LAI estimating.

Even though mono-angular imageries work in many cases, recent use of the multi-angular observation has increasingly raised concerns for accurately describing vegetation structure or landscape heterogeneity. Pocewicz et al. (2007) used the multi-angle imaging spectroradiometer (MISR) sensor data to determine whether it could improve the estimation of LAI across a post-fire ponderosa pine forest located in the Black Hills of South Dakota. They found that the relationships between the normalized difference vegetation index (NDVI) or the enhanced vegetation index (EVI) and LAI showed little variation across view angles when the understory vegetation was senesced and significant anisotropy when understory green LAI was the greatest. Verrelst et al. (2008) used the Compact High Resolution Imaging Spectrometer onboard the Project for On-Board Autonomy (CHRIS/PROBA) which provided multi-angular data to assess the reflectance anisotropy of broadband, as well as narrowband indices for pine forest and meadow of the eastern Ofenpass valley, Switzerland. Their results highlighted the influence of viewing geometry and surface reflectance anisotropy, particularly when using light use efficiency and leaf pigment indices. Fan et al. (2010) also used CHRIS/PROBA data to inverse LAI via a directional second derivative (DSD) method in Zhangye, Gansu Province, China, and demonstrated that the method was accurate and effective with the aid of the innovative filtering method.

In short, both near zenith angle and multi-angular data have been investigated for LAI estimation, while the sensitivity analyses of LAI inversion to multi-angular remote sensing imageries have been relatively less documented, thus hindering the efficiency and reliability of LAI estimation. The objective of this study is to investigate the sensitivity of LAI estimation to the variation of vegetation indices from five observation angles using CHRIS/PROBA data. To achieve this, the relationship models were established between five vegetation indices from each of the five observation angles and LAIs of five vegetation types. The sensitivities were then calculated and compared for each of the vegetation types and vegetation indices, respectively.

2 Materials and methods

2.1 Study area and data source

The study area was located in Yugan County, Jiangxi Province, China (116°13′45″–116°54′24″E, 28°21′36″–29°3′24″N) (Fig. 1), measuring at approximately 280 km^2. The terrain is composed mainly of hills and low mountains (average elevation about 80 m). The area is in a subtropical humid climate zone with an average annual temperature of 18°C and annual precipitation of 1,341 mm. The greatest concentration of rainfall occurs from April to June. The *Pinus massoniana* prevails in the area. Five vegetation communities were measured, including grass (GR), shrub (SH), coniferous forest (CF), coniferous-broadleaf forest (CB), and broadleaf forest (BF). The main vegetation species of the sampling sites are *Dicranopteris dichotoma*, *Woodwardia japonica*, *Camellia oleifera*, *Schima superba*, *Pinus raassoniana*, *Schima superba*, and *Cunninghamia lanceolata*. The sampling sites are primarily distributed in low hilly areas.

The imagery data of this study are CHRIS/PROBA acquired on May 11, 2008 (http://glovis.usgs.gov/). The CHRIS sensor on PROBA provides co-registered, spectral contiguous bands at 17 m ground sampling distance, in the spectral wavelength ranging from 400 nm to 1,050 nm. PROBA is an experimental space platform of the European Space Agency (ESA) which enables the sensor to capture images from five viewing angles. CHRIS Mode 3 (Land) data were acquired over the study area on May 11, 2008. Data viewing geometry is shown in Fig. 2. Solar position can be regarded as constant for all five CHRIS Fly-by Zenith Angles (FZA), since the time difference between the first and last recording during the satellite overpass was less than two minutes. In the current along-track pointing configuration, the FZA deviated more or less from the actual observation angle. The nominal nadir scene was 3.84° in the backward direction, the forward FZA + 36° and + 55° were 28.6° and 50.6°, respectively, and the backward FZA −36° and −55° were 33.8° and 53.5°, respectively.

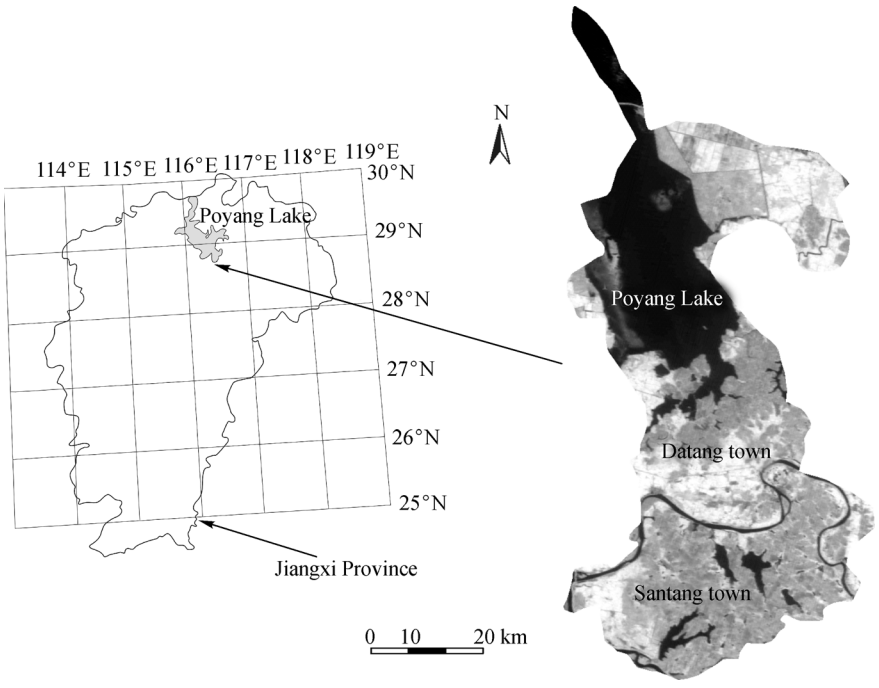

Fig. 1 Location of the study area of Jiangxi Province, China. The background of the study area is one near-infrared band (band14) of the CHRIS/PROBA data acquired on May 11, 2008.

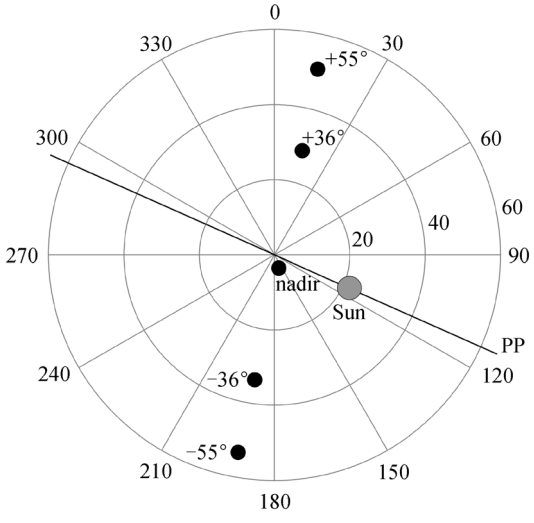

Fig. 2 Polar plot of CHRIS/PROBA data acquisition and illumination geometry. PP: Principal Plane.

2.2 Field measurement of LAI

According to accessibility, perceived representation, and being relatively undisturbed (Ringrose et al., 2003), a total of 100 quadrats were configured with the aid of relief and land-use maps. The quadrats for GR, SH, CF, CB, and BF were 40, 8, 29, 12, and 11, respectively. The precise locations of the quadrats were determined using a Starlink Invicta 210 difference GPS receiver (RAVEN Industries, Inc., USA).

LAI measurements were carried out with an LAI-2000 vegetation canopy analyzer (Li-COR, Lincoln, NE). Measurements were taken in June 2011, under uniform diffuse skies. Due to the three year lag between the field measurement and the acquirement of the CHRIS/PROBA image, the 100 quadrats were selected on the sites without obvious human intervention for years. Each quadrat measured 20 m×20 m, close to the resolution of the remote sensing image (17 m). To conduct the measurements, the LAI analyzer was positioned in an open site

close to the quadrats (< 200 m) to collect reference-sky readings, and was then carried under each plot canopy to measure light transmission through the canopy. The analyzer was covered with a 270° view cap. Approximately five to eight below-canopy samples were taken, at points about 2 to 3 m along two parallel transects, and spaced by 10 m. The LAI values of a quadrat were calculated by averaging all internal measurements. Statistics of the measurement are shown in Table 1.

2.3 Image preprocessing and VI derivation

CHRIS products are provided in top of the atmosphere (TOA) radiance, i.e., radiometrically calibrated data. In addition to typical random noise, CHRIS hyper-spectral images are affected by non-periodic, partially deterministic disturbance patterns coming from the image formation process. Meanwhile, the multi-angular CHRIS observation introduces strong perspective distortions, especially for the first and last images with larger observation zenith angles. Consequently, the noise reduction, cloud screening, atmospheric correction, and geometric correction were in turn carried out for image preprocessing using the software BEAM, a toolbox funded by the European Space Agency (ESA). The noise reduction tool was first used to correct and remove the coherent noises, known as drop-outs and vertical striping. Secondly, the cloud screening tool was used to mask cloudy pixels in CHRIS images. Thirdly, the TOA radiance was converted to surface reflectance images via the atmospheric correction tool in an automated manner, using the columnar water vapor derived for CHRIS acquisition mode 3. Lastly, the geometric correction was applied based on the parametric modeling of the acquisition process. The coordinates map was used for the rectification of the images, aided by 15 ground control points (GCP) acquired through the field measurement. All the CHRIS bands were rectified to the WGS-84 coordinate system.

To derive vegetation index (VI) for each measurement point, a vector file (.shp) was formed with the WGS-84 coordinate system for all the measurement points. To reduce errors caused by location, a 20 m buffer with each point was made. Next, the band value corresponding to each point was acquired by retrieving and averaging all band values in the buffer, overlaid on each band image. The correlation coefficients between field measured LAI and each of the corresponding retrieved 18 band values were calculated. The three bands, namely bands 3, 8, and 14, which have the strongest correlation with LAI in blue, red, and near-infrared domain, were selected for vegetation index derivation. Five vegetation indices were derived (Table 2), including NDVI (Rouse et al., 1974), ratio vegetation index (RVI) (Pearson and Miller, 1972), perpendicular vegetation index (PVI) (Richardson et al., 1977), modified soil adjusted vegetation index (MSAVI) (Qi et al., 1994), and atmospheric resistance vegetation index (ARVI) (Kaufman and Tanre, 1992). They represent different categories of the many vegetation indices: NDVI is sensitive to the observation and illumination geometry; the soil adjusted indices PVI and MSAVI, and the atmospheric resistance index ARVI, take background into consideration; and the simple ratio RVI performs well in dense vegetation coverage. The image preprocessing and vegetation index derivation were carried out using the software ENVI version 4.7 (Research System, Inc., USA).

2.4 Sensitivity evaluation for LAI estimation

In order to evaluate the sensitivity of LAI estimation to the variation of vegetation indices from five angular observations, the VI-LAI relationship models were first established. In total, 60 quadrats were randomly selected for modeling and 40 quadrats were chosen for model validation. For each vegetation type and each observation angle, the linear VI-LAI relationship model was established via the least square method. The regression model is expressed as

$$y = ax + b, \tag{1}$$

where y represents VI, x is LAI, a and b are gradient and interception of the model, respectively.

The fitness of the models was calculated with the determination coefficient R^2 and root mean squared error (RMSE). The latter was computed as

$$\mathrm{RMSE} = \left(\sum_{i=1}^{n} (e_i)^2 / N \right)^{\frac{1}{2}}, \tag{2}$$

where N represents quadrat number for validation and e_i is estimation residual, meaning the difference between model

Table 1 Summary statistics of the measured vegetation leaf area index (LAI, $n = 100$)

Vegetation type	Number of observations	Min LAI	Mean LAI	Max LAI	Standard deviation of LAI
Grass (GR)	39	0.10	2.82	5.32	1.26
Shrub (SH)	8	0.72	2.21	5.20	1.37
Coniferous forest (CF)	30	0.62	1.92	4.54	1.32
Conifer-broad-leaf forest (CB)	12	0.26	4.00	6.44	2.26
Broad-leaf forest (BF)	11	0.57	4.99	8.11	2.09

Table 2 Overview of selected vegetation indices

Abbreviation	Name	Formula	Reference
NDVI	Normalized difference vegetation index	$(R_{NIR}-R_{RED})/(R_{NIR}+R_{RED})$	Rouse et al., 1974
RVI	Ratio vegetation index	R_{NIR}/R_{RED}	Pearson and Miller, 1972
MSAVI	Modified soil adjusted vegetation index	$\frac{2R_{NIR}+1-\sqrt{(2R_{NIR}+1)^2-8(R_{NIR}-R_{RED})}}{2}$	Qi et al., 1994
PVI	Perpendicular vegetation index	$\sqrt{(0.355R_{NIR}-0.149R_{RED})^2+(0.355R_{RED}-0.852R_{NIR})^2}$	Richardson and Wiegand, 1977
ARVI	Atmospherically resistant vegetation index	$\frac{R_{NIR}-(2R_{RED}-R_{BLUE})}{R_{NIR}+(2R_{RED}-R_{BLUE})}$	Kaufman and Tanre, 1992

estimated VI and image derived VI at quadrat *i*. The modeling and validation was carried out using the software SPSS version 17.0 (SPSS Inc., USA).

The sensitivity of LAI estimation to the variation of vegetation indices was then evaluated by Eq. (3) according to Gonsamo and Pellikka (2012):

$$\mathrm{LAI_s} = \frac{a}{\mathrm{RMSE}}, \quad (3)$$

where *a* is the first derivative (gradient) of the linear regression model established using Eq. (1).

3 Results and discussion

3.1 VI- LAI relationship model

Based on 60 modeling data, a total of 125 VI-LAI linear relationship models were established for each vegetation type and observation angle. The best-fit models of each vegetation type are based on RVI, as shown in Table 3.

For each vegetation type, the mean R^2 value of each of the 25 models ranked as CB (0.866) > BF (0.795) > CF (0.579) > SH (0.556) > GR (0.162), indicating that the VI-LAI models are more reliable for taller trees than for low-growing shrub-grasses, and are more reliable for forest with broad leaf trees than for coniferous forest. For each observation angle, the greatest average R^2 values of each of the 25 models is + 55° (0.609), followed by 0° (0.591), + 36° (0.572), and − 36° (0.561), and the R^2 for − 55° (0.551) is the lowest, suggesting that the forward angles are more reliable than backward angles for LAI estimation. For each VI, RVI has the highest mean R^2 (0.652) of the 25 models, followed by NDVI (0.610), MSAVI (0.577), and PVI (0.538). The lowest mean R^2 is ARVI (0.508), implying that the VI-LAI models are the most reliable based on the traditionally used ratio-dependent vegetation indices RVI and NDVI, while the background (soil and atmosphere) modified VIs did not perform as well as we had expected.

3.2 Sensitivity of LAI estimation for different vegetation type

For each vegetation type, the sensitivity of LAI estimation to the variation of VIs from different observation angles ($\mathrm{LAI_s}$) is shown in Fig. 3. The mean $\mathrm{LAI_s}$ of five vegetation types are in the rank of BF (22.507) > CB (9.194) > CF (7.812) > SH (4.032) > GR (3.015), indicating that, similar to model R^2, the sensitivity depends on both the vegetation height and the leaf size. The greater the forest height and leaf size, the greater the sensitivity for estimating LAI: the LAIs of CB and BF are the highest (especially at + 55°), followed by CF, GR, and SH, which are the lowest. The tree height and leaf size essentially represent vegetation structure and spatial distribution of

Table 3 The best-fit VI-LAI models for each vegetation type

Observation angle	Vegetation type	Model	R^2
+ 55°	GR	$y = 0.0199x + 0.1056$	0.325
+ 55°	SH	$y = 0.0178x + 0.0622$	0.860
0°	CF	$y = 0.2769x + 1.5840$	0.597
0°	CB	$y = 0.0162x + 0.0996$	0.979
0°	BF	$y = 0.9110x + 0.1394$	0.919

Note: GR, SH, CF, CB, and BF mean grass, shrub, coniferous forest, conifer-broad-leaf forest, and broad-leaf forest, respectively. *y* is ratio vegetation index (RVI), *x* is leaf area index (LAI).

forests, which are generally characterized by heterogeneity of vertical profile, vegetation species, crown shape, and stand density (Pinty et al., 2002; Nolin, 2004; Rautiainen et al., 2004, 2008). The heterogeneity of forests complicates the properties of quadrat reflectivity, thus differentiates the response of VIs from multi-angular observation. More oblique observation potentially increases the observed heterogeneity of the vegetation communities with broad-leaf trees (CB and BF, Figs. 3(d) and 3(e)), resulting in the highest sensitivity among all observation angles. These findings are consistent with the previous study of Heiskanen (2006). In contrast, all five angles show similar sensitivities for coniferous forest (Fig. 3(d)). This may mainly be due to the relatively low vegetation density and simple structures of such communities, which lead to a lesser difference among observed components, and thus similar sensitivities. In the same manner, the relatively simple and homogenous grass and shrub communities result in less sensitive behavior of angular VIs (Figs. 3(a) and 3(b)). Moreover, the backward observations ($-36°$ and $-55°$) have generally low sensitivities, significantly different from those in forward observations ($+36°$ and $+55°$) for vegetation communities with broad-leaf trees (CB and BF). At this time it is difficult for us to explicitly explain the mechanism of such phenomenon, which is most likely due to the difference between observed structures of the vegetation communities from forward and backward perspectives.

3.3 Sensitivity of LAI estimation for different VI

The LAI_s for each VI is shown in Fig. 4. The mean LAI_s of

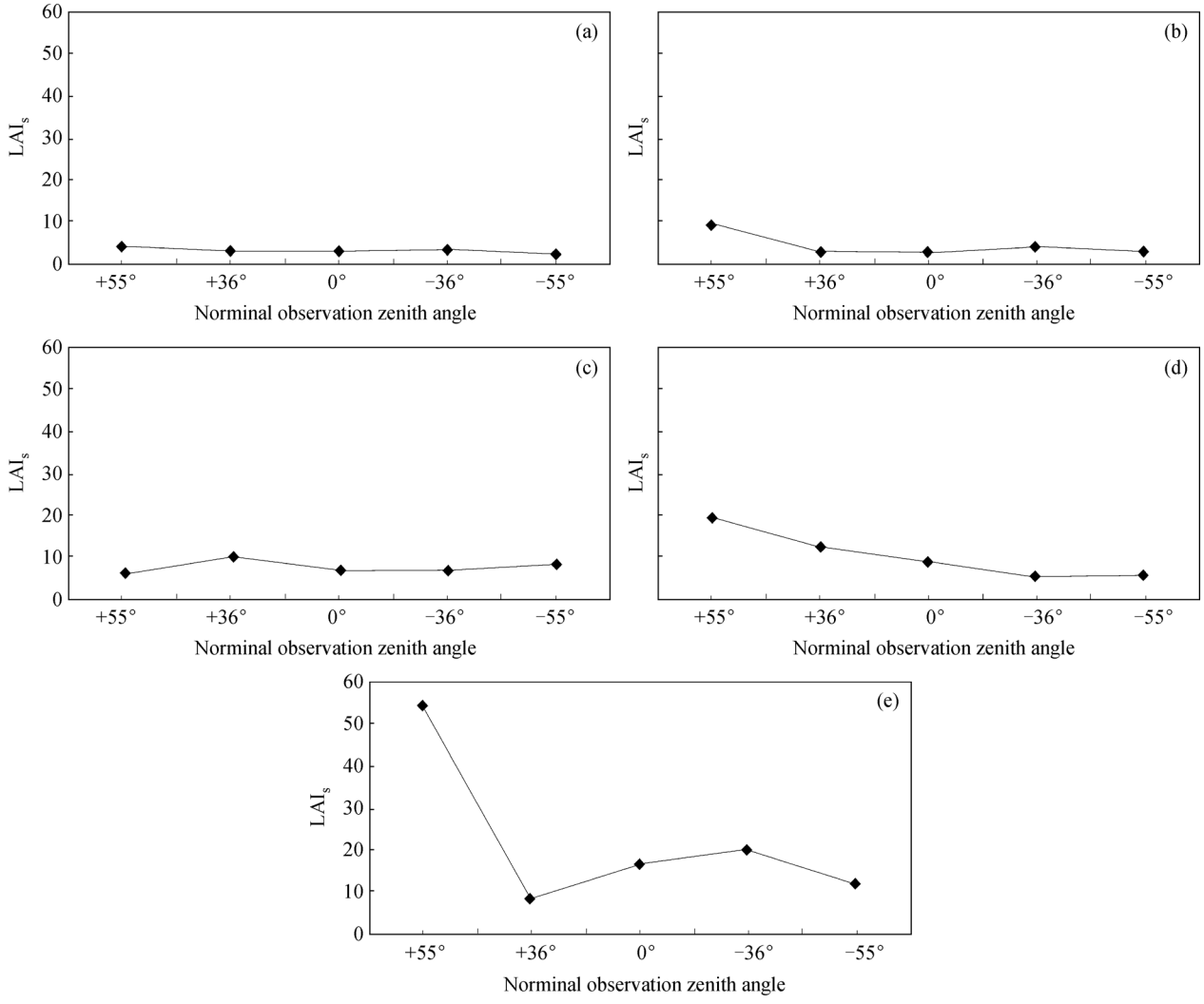

Fig. 3 Mean LAI_s of: (a) grass (GR), (b) shrub (SH), (c) coniferous forest (CF), (d) conifer-broad-leaf forest (CB), and (e) broad-leaf forest (BF). LAI_s is the sensitivity of LAI estimation to the variation of vegetation indices from different observation angles. *X*-axis denotes norminal observation zenith angle, where positive and negative angles mean forward and backward observation (besides the nadir), respectively.

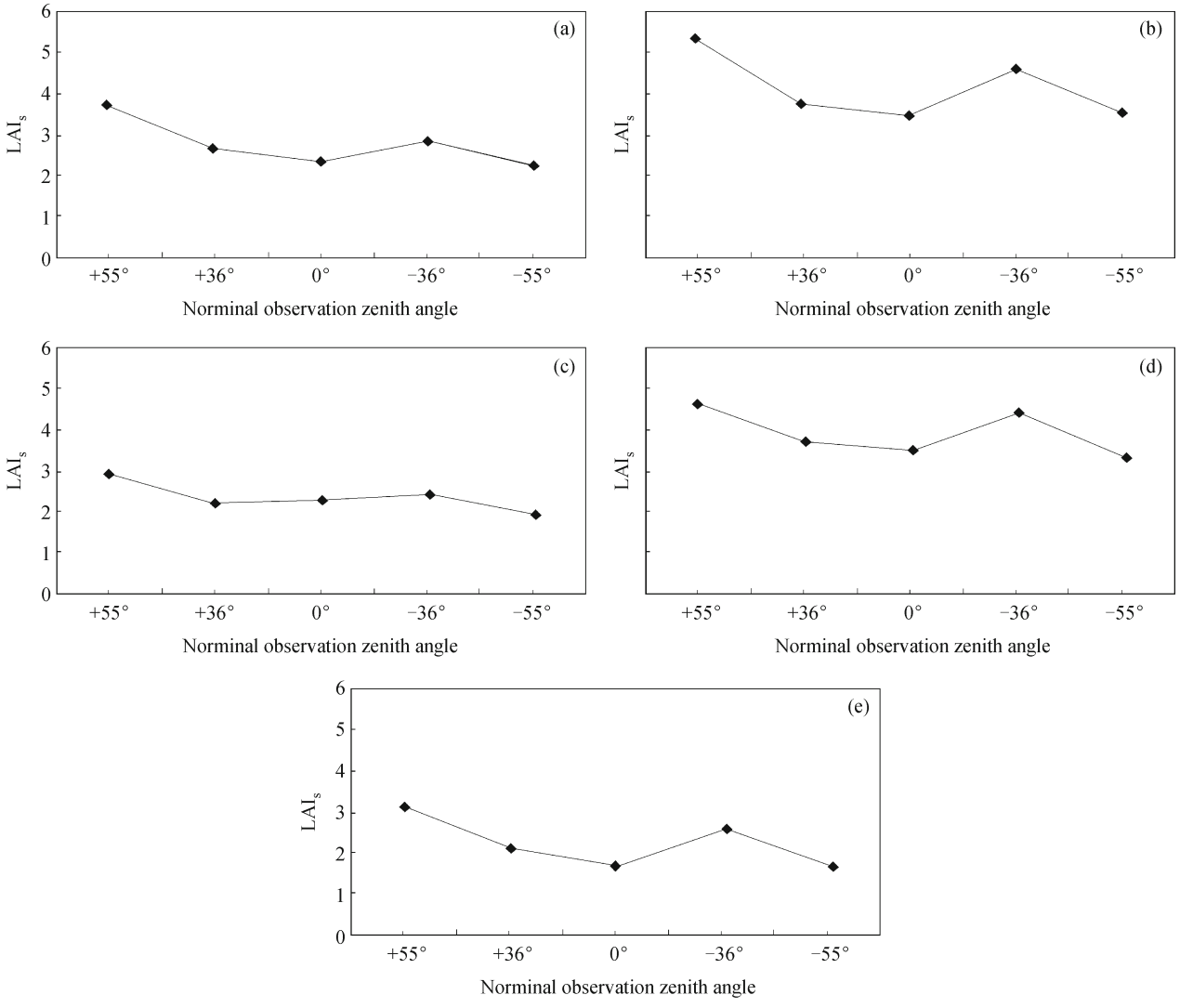

Fig. 4 Mean LAI_s of: (a) NDVI, (b) RVI, (c) MSAVI, (d) PVI, and (e) ARVI. LAI_s is the sensitivity of LAI estimation to the variation of vegetation indices from different observation angles. *X*-axis denotes norminal observation zenith angle, where positive and negative angles mean forward and backward observation (besides the nadir), respectively.

five VIs is in the rank of RVI (4.177) > NDVI (3.844) > PVI (2.773) > MSAVI (2.398) > ARVI (2.206), showing that for LAI estimation, the commonly used RVI and NDVI are most sensitive to LAI, while the indices involving background soil or atmospheric conditions are just the opposite. A similar result was observed by Jin et al. (2002) and Abdou et al. (2006) when using the surface Bidirectional Reflectance Factor (BRF) products of a Special session on Multi-angle Remote Sensing (MISR) data. It seems that the correction of background noise blunts the sensitivities of VIs to LAIs, which is quite a surprise compared with literature-based acknowledged findings. As far as we know, a more accurate understanding is that, the background (soil or atmosphere) adjust parameters used in our study were based on (near) nadir observation, which has been routinely applied in traditional researches. The contribution of background soil and atmosphere may potentially have different angle-related patterns to observed reflectance, requiring different ways to modify so as to effectively reduce its influence and minimize the noise. The multi-angular soil and/or atmosphere adjust parameters may hopefully improve the performance of the VIs in LAI estimation, necessitating further investigation as part of our future work. In addition, the observation angle has similar effects on the sensitivity analyses in terms of VI compared with vegetation type as shown above: highest LAI_s at + 55°, but lowest at −55°, interestingly requiring further insights into the relationships between solar incidence, vegetation structure, and multi-angular remote sensing.

4 Conclusions

In this study, the sensitivity of LAI estimation to the variation of VI from observation angles was analyzed. The following conclusions can be drawn:

1) The VI-LAI models are more reliable for taller trees than for low-growing shrub-grasses, better for forests with broad leaf trees than for coniferous forest, and optimal with traditionally used RVI and NDVI, rather than with the background (soil and atmosphere) modified VIs in this study.

2) The sensitivity of LAI estimation to VIs from multi-angular observation depends mainly on the heterogeneity of vegetation communities. The greater the forest height and leaf size, the greater the sensitivity. Forests with broad-leaf trees have higher sensitivities, especially at oblique angles, while relatively simple-structured coniferous forest, shrub, and grass show similar sensitivities at all angles.

3) In LAI estimation, the commonly used RVIs and NDVIs are most sensitive to LAI. The multi-angular soil and/or atmosphere adjust parameters may hopefully improve the performance of the VIs in LAI estimation, requiring our further investigation.

Acknowledgements This research was funded by the National Natural Science Foundation of China (Grant No. 41071281), the Natural Science Foundation of Jiangsu Province (No. BK20131078), the Qing Lan Project of Jiangsu Provincial Department of Education, and the Natural Science Foundation of Jiangsu Provincial Department of Education, China (10KJD170005). The authors are very grateful to the anonymous referees for their comments given for the improvement of the manuscript.

References

Abdou W A, Pilorz S H, Helmlinger M C, Conel J E, Diner D J, Bruegge C J, Martonchik J V, Gatebe C K, King M D, Hobbs P V (2006). Sua pan surface bidirectional reflectance: a case study to evaluate the effect of atmospheric correction on the surface products of the Multi-angle Imaging Spectro Radiometer (MISR) during SAFARI 2000. IEEE Trans Geosci Rem Sens, 44(7): 1699–1706

Baret F, Guyot G (1991). Potentials and limits of vegetation indices for LAI and APAR assessment. Remote Sens Environ, 35(2–3): 161–173

Bonan G B (1995). Land-atmosphere interactions for climate system models: coupling biophysical, biogeochemical, and ecosystem dynamical processes. Remote Sens Environ, 51(1): 57–73

Chen J M, Black T A (1992). Defining leaf area index for non-flat leaves. Plant Cell Environ, 15(4): 421–429

Chen J M, Pavlic G, Brown L, Cihlar J, Leblac S G, White H P, Hall R J, Peddle D R, King D J, Trofymow J A, Swift E, van der Sanden J, Pellikka P K E (2002). Derivation and validation of Canada-wide coarse-resolution leaf area index maps using high resolution satellite imagery and ground measurement. Remote Sens Environ, 80(1): 165–184

Cohen W B, Maiersperger T K, Gower S T, Turner D P (2003). An improved strategy for regression of biophysical variables and Landsat ETM + data. Remote Sens Environ, 84(4): 561–571

Colombo R, Dario B, Dante F, Carlo M M (2003). Retrieval of leaf area index in different vegetation types using high resolution satellite data. Remote Sens Environ, 86(1): 120–131

Darvishzadeh R, Skidmore A, Schlerf M, Atzberger C (2008). Inversion of a radiative transfer model for estimating vegetation LAI and chlorophyll in a heterogeneous grassland. Remote Sens Environ, 112 (5): 2592–2604

Duan A W (1996). Measuring leaf area index of crop colony. Irrigation and Drainage Systems, 15: 50–53

Fan W J, Xu X R, Liu X C, Yan B Y, Cui Y K (2010). Accurate LAI retrieval method based on PROBA/CHRIS data. Hydrol Earth Syst Sci, 14(8): 1499–1507

Fernandes R, Butson C, Leblanc S, Latifovic R (2003). Landsat-5 TM and Landsat-7 ETM + based accuracy assessment of leaf area index products for Canada derived from SPOT-4 VEGETATION data. Can J Rem Sens, 29(2): 241–258

Fernández N, Paruelo J M, Delibes M (2010). Ecosystem functioning of protected and altered Mediterranean environments: a remote sensing classification in Doñana, Spain. Remote Sens Environ, 114(1): 211–220

Ganguly S, Schull M A, Samanta A, Shabanov N V, Milesi C, Nemani R R, Knyazikhin Y, Myneni R B (2008). Generating vegetation leaf area index earth system data record from multiple sensors. Part 1: Theory. Remote Sens Environ, 112(12): 4333–4343

Gonsamo A, Pellikka P (2012). The sensitivity based estimation of leaf area index from spectral vegetation indices. ISPRS J Photogramm Remote Sens, 70: 15–25

Gower S T, Kucharik C J, Norman J M (1999). Direct and indirect estimation of leaf area index, fAPAR and net production of terrestrial ecosystem. Remote Sens Environ, 70(1): 29–51

Gu Z J, Ju W M, Liu Y B, Li D Q, Fan W L (2012). Applicability of spectral and spatial information from IKONOS-2 Imagery in retrieving Leaf Area Index of forests in the urban area of Nanjing, China. J Appl Remote Sens, 6(1): 063556-1

Gu Z J, Shi X Z, Li L, Yu D S, Liu L S, Zhang W T (2011). Using multiple radiometric correction images to estimate leaf area index. Int J Remote Sens, 32(24): 9441–9454

Heiskanen J (2006). Tree cover and height estimation in the Fennoscandian tundra–taiga transition zone using multiangular MISR data. Remote Sens Environ, 103(1): 97–114

Houborg R, Soegaard H, Boegh E (2007). Combining vegetation index and model inversion methods for the extraction of key vegetation biophysical parameters using Terra and Aqua MODIS reflectance data. Remote Sens Environ, 106(1): 39–58

Hyer E J, Goetz S J (2004). Comparison and sensitivity analysis of instruments and radiometric methods for LAI estimation: assessments from a boreal forest site. Agric Meteorol, 122(3–4): 157–174

Jin Y F, Gao F, Schaaf C B, Li X W, Strahler A H, Bruegge C J, Martonchik J V (2002). Improving MODIS surface BRDF/albedo retrieval with MISR multiangle observation. IEEE Trans Geosci Rem Sens, 40(7): 1593–1604

Kaufman Y J, Tanre D (1992). Atmospherically resistant vegetation index (ARVI) for EOS-MODIS. Geoscience and Remote Sensing, IEEE Transactions on, 30(2): 261–270

McAllister D M, Valeo C A (2007). Robust new method for the remote

estimation of LAI in montane and boreal forests. Int J Remote Sens, 28(8): 1891–1905

Nolin A W (2004). Towards retrieval of forest cover density over snow from the Multi-angle Imaging SpectroRadiometer (MISR). Hydrol Processes, 18(18): 3623–3636

Pearson R L, Miller L D (1972). Remote mapping of standing crop biomass for estimation of the productivity of the shortgrass prairie. Proceedings of the Eighth International symposium on Remote Sensing of the Environment, VIII: 1355–1379

Pinty B, Widlowski J L, Gobron N, Verstraete M M, Diner D J (2002). Uniqueness of multiangular measurements. I: an indicator of subpixel surface heterogeneity from MISR. IEEE Trans Geosci Rem Sens, 40 (7): 1560–1573

Pocewicz A, Vierling L A, Lentile L B, Smith R (2007). View angle effects on relationships between MISR vegetation indices and leaf area index in a recently burned ponderosa pine forest. Remote Sens Environ, 107(1–2): 322–333

Qi J, Chehbouni A, Huete A R, Kerr Y H, Sorooshian S (1994). A modified soil adjusted vegetation index. Remote Sens Environ, 48(2): 119–126

Rautiainen M, Lang M, Mottus M, Kuusk A, Nilson T, Kuusk J, Lukk T (2008). Multi-angular reflectance properties of a hemiboreal forest: an analysis using CHRIS PROBA data. Remote Sens Environ, 112 (5): 2627–2642

Rautiainen M, Stenberg P, Nilson T, Kuusk A (2004). The effect of crown shape on the reflectance of coniferous stands. Remote Sens Environ, 89(1): 41–52

Richardson A J, Wiegand C L (1977). Distinguishing vegetation from soil background information. Am Soc Photogrammetric Rem Sens, 43(12): 1541–1552

Ringrose S, Matheson W, Wolski P, Huntsman-Mapila P (2003). Vegetation cover trends along the Botswana Kalahari transect. J Arid Environ, 54(2): 297–317

Rouse J W, Haas R H, Schell J A, Deering D W, Harlan J C (1974). Monitoring the vernal advancement of retrogradation of natural vegetation. Greenbelt, MD: NASA/GSFC (Type III, Final Report), 371

Running S W, Nemani R, Peterson D L, Band L E, Potts D F, Pierce L L, Spanner M A (1989). Mapping regional forest evapotranspiration and photosynthesis by coupling satellite data with ecosystem simulation. Ecology, 70(4): 1090–1101

Smith B, Knorr W, Widlowski J L, Pinty B, Gobron N (2008). Combining remote sensing data with process modelling to monitor boreal conifer forest carbon balances. For Ecol Manage, 255(12): 3985–3994

Verrelst J, Schaepman M E, Koetz B, Kneubuhler M (2008). Angular sensitivity analysis of vegetation indices derived from CHRIS/ PROBA data. Remote Sens Environ, 112: 2341–2353

Vohland M, Mader S, Dorigo W (2010). Applying different inversion techniques to retrieve stand variables of summer barley with PROSPECT + SAIL. Int J Appl Earth Obs Geoinf, 12(2): 71–80

Wu X X, Gu Z J, Luo H, Shi X Z, Yu D S (2014). Analyzing forest effects on runoff and sediment production using Leaf Area Index. J Moutain Sci, 11(1): 119–130

AUTHOR BIOGRAPHIES

Jianjun Cao earned his BSc and MSc in Environment Engineering at the China University of Mining and Technology in Xuzhou, China, in 2000 and 2004 respectively. He is currently a PhD candidate at East China Normal University in Shanghai, China. He is also an associate professor at the School of Bio-Chemical and Environmental Engineering, Nanjing Xiaozhuang University, China. His research interests include remote sensing of vegetation parameters and spatial decision support. He has published more than 20 papers on GIS and remote sensing. E-mail: jjuncaol@163.com

Zhujun Gu is currently a visiting scholar at the Earth Observation Systems Laboratory, Earth and Atmospheric Sciences Department, University of Alberta, Edmonton, Alberta, Canada. He earned a BSc in 1993, and MSc in 2005 from the School of Geographical Science at Nanjing Normal University, China, a PhD in 2008 from the State Key Laboratory of Soil and Sustainable Agriculture, Institute of Soil Science, Chinese Academy of Sciences, China, and a postdoctoral researcher at the International Institute for Earth System Sciences, Nanjing University, China. He is now an associate professor at the School of Bio-Chemical and Environmental Engineering, Nanjing Xiaozhuang University, China. His areas of interest include remote sensing of forest structures, ecological monitoring and evaluation, and soil and water conservation.